Research Square

Preprints are preliminary reports that have not undergone peer review.
They should not be considered conclusive, used to inform clinical practice,
or referenced by the media as validated information.

Subthalamic stimulation reduces loss weighting and prospective confidence while strengthening feedback–mood coupling

Julien Bastin

julien.bastin@univ-grenoble-alpes.fr

Univ. Grenoble Alpes, Inserm, U1216, Grenoble Institut Neurosciences, GIN https://orcid.org/0000-0002-0533-7564

Audrey Kist

Univ. Grenoble Alpes, Inserm, U1216, Grenoble Institut Neurosciences, GIN

Romane Cecchi

École Normale Supérieure, Université Paris Sciences et Lettres, INSERM U960 https://orcid.org/0000-0002-6149-939X

Elodie Blouzard

Univ. Grenoble Alpes, Inserm, U1216, Grenoble Institut Neurosciences, GIN

Arnaud Pouchon

Univ. Grenoble Alpes, Inserm, U1216, Grenoble Institut Neurosciences, GIN

Stephan Chabardes

Univ. Grenoble Alpes, Inserm, U1216, Grenoble Institut Neurosciences, GIN

Nathan Faivre

Université Grenoble Alpes https://orcid.org/0000-0001-6011-4921

Michael Pereira

INSERM https://orcid.org/0000-0003-0778-674X

Mircea Polosan

Univ. Grenoble Alpes, Inserm, U1216, Grenoble Institut Neurosciences, GIN

Article

Keywords:

Posted Date: November 12th, 2026

DOI: https://doi.org/10.21203/rs.3.rs-11692438/v1

License: This work is licensed under a Creative Commons Attribution 4.0 International License.
Read Full License

Additional Declarations: There is **NO** Competing Interest.

Subthalamic stimulation reduces loss weighting and prospective confidence while strengthening feedback–mood coupling

Audrey Kist[1,2], Romane Cecchi[1,3], Elodie Blouzard[1], Arnaud Pouchon[1,4], Stephan Chabardès[1,5,6], Nathan Faivre[2], Michael Pereira[1], Mircea Polosan[1,4], Julien Bastin[1]

[1] Univ. Grenoble Alpes, Inserm, U1216, Grenoble Institut Neurosciences, 38000 Grenoble, France
[2] Univ. Grenoble Alpes, Univ. Savoie Mont Blanc, CNRS, LPNC, 38000 Grenoble, France
[3] Laboratoire de Neurosciences Cognitives et Computationnelles (LNC²), Département d'Études Cognitives, École Normale Supérieure, Université PSL, INSERM, 75005 Paris, France
[4] Department of Psychiatry, CHU Grenoble Alpes, 38000 Grenoble, France
[5] Univ. Grenoble Alpes, Inserm, Department of Neurosurgery, 38000, Grenoble, France
[6] Univ. Grenoble Alpes, CEA, LETI, Clinatec, 38000, Grenoble, France

Corresponding author: Julien.bastin@univ-grenoble-alpes.fr

ABSTRACT

Deciding how much to stake on future performance involves anticipating success or failure, while outcomes shape momentary mood. Yet little is known about how the antero-ventro-medial subthalamic nucleus (avmSTN) contributes to these processes. We studied 13 patients with obsessive–compulsive disorder in a randomized, double-blind crossover design with avmSTN stimulation ON and OFF. Participants accepted or rejected monetary offers before performing a visuomotor challenge, reporting prospective confidence and intermittent mood level. A computational choice model revealed lower loss weighting during avmSTN stimulation. Stimulation was also associated with lower prospective confidence, particularly for accepted offers, and a stronger relationship between monetary feedback and reported mood. These findings suggest that stimulation avmSTN circuitry influences prospective self-evaluation and outcome-related affect, with a model-dependent effect on loss valuation. These findings reveal how associative-limbic subthalamic stimulation modulates distinct subprocesses of motivated behavior, linking model-based valuation to prospective self-evaluation and outcome-related affect.

Keywords: obsessive compulsive disorder; deep brain stimulation; subthalamic nucleus; choice; mood; confidence.

INTRODUCTION

Obsessive-compulsive disorder (OCD) affects up to 1.7% of the population and is characterized by intrusive thoughts (obsessions) and compulsive behaviors that can severely impair daily functioning and quality of life [1]. Although behavioral therapy and serotonin reuptake inhibitors provide relief for many patients, a substantial subset (10–20%) remains treatment-refractory. In these severe cases, deep brain stimulation (DBS) targeting the subthalamic nucleus (STN) can substantially reduce symptom severity [2]. Yet, the therapeutic efficacy of STN–DBS contrasts with our limited understanding of how stimulation alters the cognitive and affective processes that guide behavior. This gap is particularly relevant because OCD has been associated with altered anticipation and processing of aversive outcomes [3], as well as abnormal confidence and uncertainty judgments [4–6]. Determining how STN stimulation affects these processes may therefore provide insight into both the functional role of this region and the mechanisms through which DBS modifies behavior in OCD.

Most of the existing human evidence about the functional role of the human STN during motivational processes comes from studies of STN-DBS in Parkinson's disease (PD). STN low-frequency oscillations have been related to the subjective perception of rewards and effort [7,8] while STN–DBS can alter cost–benefit decisions and risky choice [9,10]. Recent work further emphasizes that these effects cannot necessarily be reduced to a unitary change in risk attitude or impulsivity, as prospective gains and losses, uncertainty, and subjective risk-taking tendencies can be dissociated behaviorally and physiologically [11]. Beyond decision-making, STN stimulation can also acutely alter affective states, with early case reports describing stimulation-induced mirthful laughter and hypomanic behavior in PD [12]. Two important factors, however, limit the generalization of findings from PD to OCD. First, PD is characterized by profound alterations of the dopaminergic system, which may influence how STN stimulation modulates behavior. Second, DBS for PD primarily targets the dorsolateral sensorimotor STN, whereas DBS for OCD targets its anterior ventro-medial (avmSTN) portion which corresponds to its associative–limbic territory, characterized by distinct connectivity and functional properties [13,14].

Direct evidence concerning the contribution of the avmSTN to these processes in OCD remains scarce. STN–DBS in OCD has been shown to alter decisional impulsivity, reducing evidence accumulation under probabilistic uncertainty and increasing delay discounting, without altering subjective confidence [15]. Subsequent work showed that STN–DBS produced dissociable effects on reward- and loss-related decisions, decreasing risky choices for prospective rewards while

reducing sensitivity to the magnitude of prospective losses [16]. Converging evidence also implicates the same STN territory in uncertainty-related and affective processes. Single-neuron activity in the avmSTN is modulated during doubt and checking behavior [17], while STN theta-band activity has been associated with emotional states in PD and OCD [18]. Stimulation of this territory modulates affective states [19] and, in some cases, induce hypomania [2]. These observations suggest that avmSTN stimulation may influence multiple processes that shape decision-making, rather than a single decision variable.

One way to operationalize the affective state relevant to ongoing decisions is through momentary subjective well-being, or mood, which can be modeled as a dynamically changing internal state shaped by the recent history of positive and negative feedback [20–22]. Importantly, these feedback-driven fluctuations appear to be specific to mood rather than reflecting a general change in self-evaluation: in Vinckier et al. (2018), feedback history predicted momentary mood but not prospective confidence in succeeding in an upcoming motor challenge. At the neural level, high and low mood were associated with opposite changes in baseline activity within the vmPFC and anterior insula, respectively, which in turn biased the weighting of prospective gains and losses during choice [22]. This mechanism was subsequently supported by intracerebral recordings showing that vmPFC and dorsal anterior insula broadband gamma activity tracked high and low mood and predicted increased weighting of gains and losses, respectively [23]. Together, these findings indicate that momentary subjective well-being can influence valuation and choice while remaining dissociable from prospective confidence. Whether avmSTN stimulation modulates these dimensions in parallel or selectively remains unknown.

To address this question, we studied 13 patients with severe, treatment-refractory OCD using a within-subject avmSTN-DBS ON/OFF design and included 17 healthy participants as a control group. Participants decided whether to accept a cognitive challenge associated with varying prospective monetary gains and losses, allowing us to computationally dissociate the subjective weighting of gains and losses. Choice was combined with prospective confidence ratings and intermittent ratings of momentary subjective well-being. By manipulating avmSTN stimulation while quantifying these dimensions within the same individuals, we tested whether the avmSTN exerts parallel or dissociable causal influences on valuation, prospective confidence, and momentary well-being.

RESULTS

Patients had received chronic avmSTN-DBS for at least one year before the experiment (mean stimulation duration: 6.7 ± 1.48 years). Chronic stimulation was associated with a marked reduction in OCD symptom severity, with total Y-BOCS scores decreasing from 33.5 ± 0.72 before surgery to 13.4 ± 1.63 during the initial clinical evaluation on day 0, while DBS was ON and before the randomized ON/OFF experimental sessions (paired two-sided t-test: $t_{(12)} = -11.9$, $p = 5.67 \times 10^{-8}$; **Fig. 1B**). Participants were subsequently tested ON and OFF stimulation on two consecutive days, in a randomized, double-blind, counterbalanced design separated by a 16-h washout period (**Fig. 1A**). Acute stimulation withdrawal did not significantly alter the clinical measures collected in the two conditions, including Y-BOCS resistance and control items, anxiety, or depression scores (all $p \geq 0.1$, **Table S2**). Electrode reconstruction confirmed that the active contacts were predominantly located within the antero-ventro-medial subregion of the STN (**Fig. 1C**).

To assess the acute effects of avmSTN-DBS on decision-making, prospective confidence and mood, patients performed the same behavioral task in the DBS ON and OFF conditions (**Fig. 1D**). Each trial comprised four successive stages. First, participants decided whether to accept or reject a multi-attribute offer combining three independently manipulated dimensions: a potential monetary gain, a potential monetary loss and the difficulty of an upcoming visuomotor timing challenge. In this challenge, participants had to stop a moving ball within a target of variable size after extrapolating the final, occluded part of its trajectory (see Methods). They then rated their prospective confidence in successfully completing the challenge, performed the challenge and received monetary feedback. Finally, in 25% of trials, participants additionally reported their current mood. This design allowed us to examine, within the same participants, how avmSTN-DBS influenced three successive behavioral readouts: choice, prospective confidence and moment-to-moment mood.

We first checked that the success during the challenge (i.e. successfully stopping the ball within the target) did not significantly differ between DBS conditions (Accuracy DBS-OFF: 0.48 ± 3.45×10^{-2}; DBS-ON: 0.46 ± 3.74×10^{-2}; $t_{(12)} = -1.21$, $p = 0.25$). Thus, the reported effects of STN-DBS on choice, confidence, and mood would not be attributable to differences in performance on the cognitive challenge across DBS conditions. A healthy control group was also tested but showed lower challenge performance than ON-DBS patients (CTR accuracy = 0.38 ± 1.88×10^{-2}, DBS-ON= 0.46 ± 3.74×10^{-2}, two-sample Welch T-test $t_{(7321.5)} = -8.01$, $p = 1.22 \times 10^{-15}$**)**. Because this performance difference could confound direct group comparisons of choice, confidence and mood, control data were not included in the primary ON–OFF DBS

analyses. They were nevertheless retained as secondary references and are reported in the Supplementary Information when informative **(Fig. S1 to S4).**

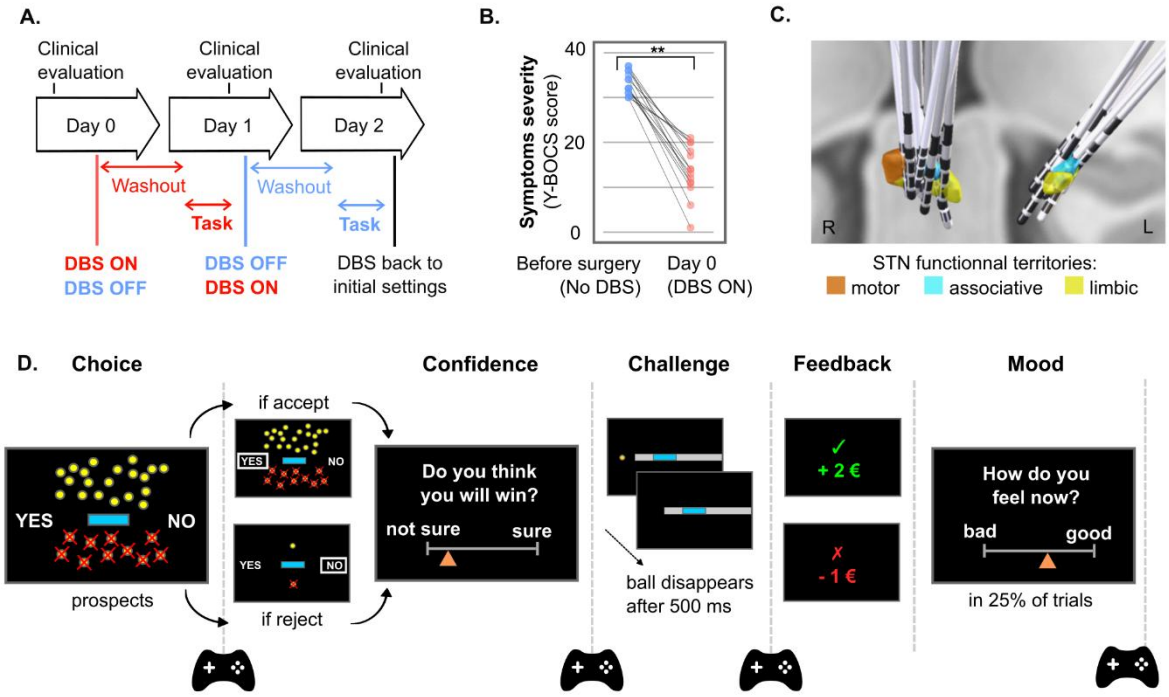


Figure 1. Experimental design. A. Double-blind procedure to assess the effects of deep brain stimulation (DBS) in patients with OCD. A 16-hour washout period separated ON vs. OFF DBS conditions. **B.** Symptoms severity for participants with OCD (Y-BOCS) before DBS surgery and ON-DBS. Stars indicate significance (paired two-sided t-test: $t_{(12)} = 11.9$, $p < 10^{-3}$). **C.** Reconstruction of DBS electrode locations. Electrodes targeted the antero-ventro-medial subregion of the subthalamic nucleus (avmSTN), encompassing associative and limbic territories. **D.** Cognitive task. During the choice phase, participants had to weigh against a default option monetary stakes (gain and loss prospects) and the difficulty of an upcoming challenge (rectangle target at screen center) to decide whether to accept a risky offer or to play for minimal stakes. Choices were followed by a prospective confidence report and thereafter by a challenge (stopping a moving dot when it reached the target). Performance feedback was displayed and finally, participants were asked to report their subjective well-being (mood) on a subset (25%) of trials.

avmSTN-DBS reduces subjective weighting of potential losses

We first examined how the three independently manipulated offer attributes (potential gain, potential loss and challenge difficulty) influenced participants' decisions to accept or reject the offer. A generalized linear mixed-effects model (GLMM) showed that acceptance probability increased with potential gain (effect estimate $\beta = 7.06 \times 10^{-2} \pm 3.98 \times 10^{-3}$, $z = 17.4$, 1.61×10^{-70}) and decreased with potential loss ($\beta = -6.80 \times 10^{-2} \pm 3.91 \times 10^{-3}$, $z = -17.3$, 8.38×10^{-68}) and challenge difficulty ($\beta = -8.36 \times 10^{-2} \pm 5.03 \times 10^{-3}$, $z = -16.6$, 5.31×10^{-62}; **Fig. 2A** and **Table S3**). Thus, participants integrated both monetary stakes and anticipated challenge difficulty when deciding whether to accept an offer. However, neither the main effect of avmSTN-DBS nor its interactions with gain, loss or difficulty significantly influenced acceptance probability (all $p > 0.05$; **Table S3**).

We next asked whether avmSTN-DBS altered latent components of the decision process that were not apparent from the model-free analysis. We fitted a previously validated computational model in which acceptance depends on the expected utility of the offer [22,23], combining potential gains and losses with the estimated probabilities of success and failure (see Methods). Separate parameters captured the subjective weights assigned to gains (k_g) and losses (k_l), while σ captured uncertainty in the internal representation of challenge performance and k_t accounted for changes in acceptance propensity over time. The model was fitted separately for each participant in the DBS ON and OFF conditions (**Fig. 2B**).

avmSTN-DBS significantly reduced the subjective weight assigned to potential losses (DBS-OFF: mean $k_l = 19.6 \pm 2.99$; DBS-ON: $k_l = 16.5 \pm 2.94$; $t_{(12)} = -2.28$, $p = 4.14 \times 10^{-2}$). No significant stimulation effect was observed for k_g, σ or k_t (**Table S4**). Thus, although stimulation did not produce a detectable change in acceptance probability in the model-free analysis, computational modeling revealed a selective reduction in the contribution of potential losses to the decision process.

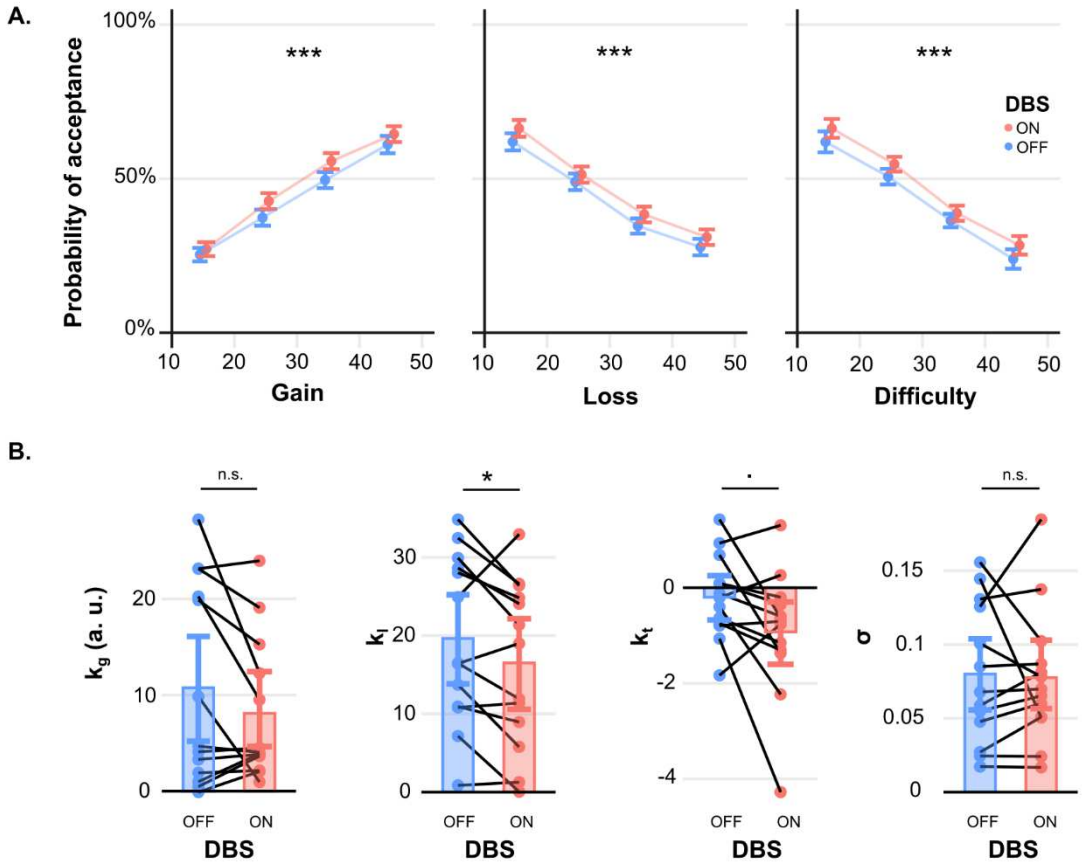


Figure 2. avmSTN DBS selectively reduces loss weighing in participants with OCD. A. Probability of accepting an offer as a function of monetary gain, monetary loss (in euro cents) and challenge difficulty (arbitrary units). Acceptance probability was significantly modulated by gain, loss and challenge difficulty, with no significant main effect of avmSTN DBS. Dots and error bars represent binned data averaged across participants ± SEM. ***P < 0.001 for the main effects of gain, loss and challenge difficulty. **B.** Choice-model parameters in the DBS OFF and ON conditions. avmSTN stimulation significantly decreased the parameter capturing the influence of prospective losses on choice (k_l), with no significant effect on the other model parameters. Dots represent individual participants, bars indicate the group mean and error bars denote the SEM. k_g, weight of prospective gains; k_l, weight of prospective losses; k_t, time-dependent drift; σ, uncertainty in the internal representation of challenge performance, representative of perceived challenge difficulty. . for p<0.1, * for $p < 5 \times 10^{-2}$, ** for $p < 10^{-2}$, *** for $p < 10^{-3}$.

avmSTN DBS reduces prospective confidence in challenge success

Before performing the challenge, participants reported whether they expected to win, providing a prospective estimate of challenge success that we refer to as prospective confidence. Confidence ratings were z-scored within each participant across sessions. We fitted a linear mixed-effects model predicting prospective confidence from prospective gain, prospective loss, challenge difficulty, accept/reject choice and DBS condition, including all interactions between DBS and choice with these task variables, and a random intercept for participant revealing significant effects among which of DBS and interactions between DBS and loss, DBS and difficulty, and DBS and acceptance (**Fig. 3A; Table S5**). Estimated marginal means showed lower prospective confidence during DBS ON than OFF (model effect estimate: $3.32 \times 10^{-1} \pm 1.59 \times 10^{-1}$, $t_{(6832)} = 2.08$, $p = 3.72 \times 10^{-2}$, difference in confidence ON − OFF = $-2.16 \times 10^{-1} \pm 2.58 \times 10^{-2}$, $z = -8.37$, $p = 5.71 \times 10^{-17}$; **Fig. 3B**; **Table S6**). This effect depended on participants' choice (DBS × choice: $\beta = -7.24 \times 10^{-1} \pm 2.27 \times 10^{-1}$, $t_{(6832)} = -3.18$, $p = 1.47 \times 10^{-3}$): DBS reduced prospective confidence both for rejected challenges (ON − OFF = -9.90×10^{-2}, $z = -2.91$, $p = 3.64 \times 10^{-3}$) and, more strongly, for accepted challenges (ON − OFF = $-3.33 \times 10^{-1} \pm 3.88 \times 10^{-2}$, $z = -8.59$, $p = 8.87 \times 10^{-18}$). The model further revealed interactions between DBS and loss prospect ($\beta = -6.48 \times 10^{-3} \pm 2.82 \times 10^{-3}$, $t_{(6832)} = -2.29$, $p = 2.18 \times 10^{-2}$) and between DBS and challenge difficulty ($\beta = -9.21 \times 10^{-3} \pm 3.46 \times 10^{-3}$, $t_{(6832)} = -2.67$, $p = 7.70 \times 10^{-3}$), indicating that stimulation altered the relationship between these task dimensions and prospective confidence. However, the corresponding marginal comparisons of loss and difficulty slopes between DBS conditions were close to the conventional significance threshold (loss: $z = -1.97$, $p = 4.88 \times 10^{-2}$; difficulty: $z = -1.93$, $p = 5.42 \times 10^{-2}$; **Table S6**). These interaction effects should therefore be interpreted cautiously.

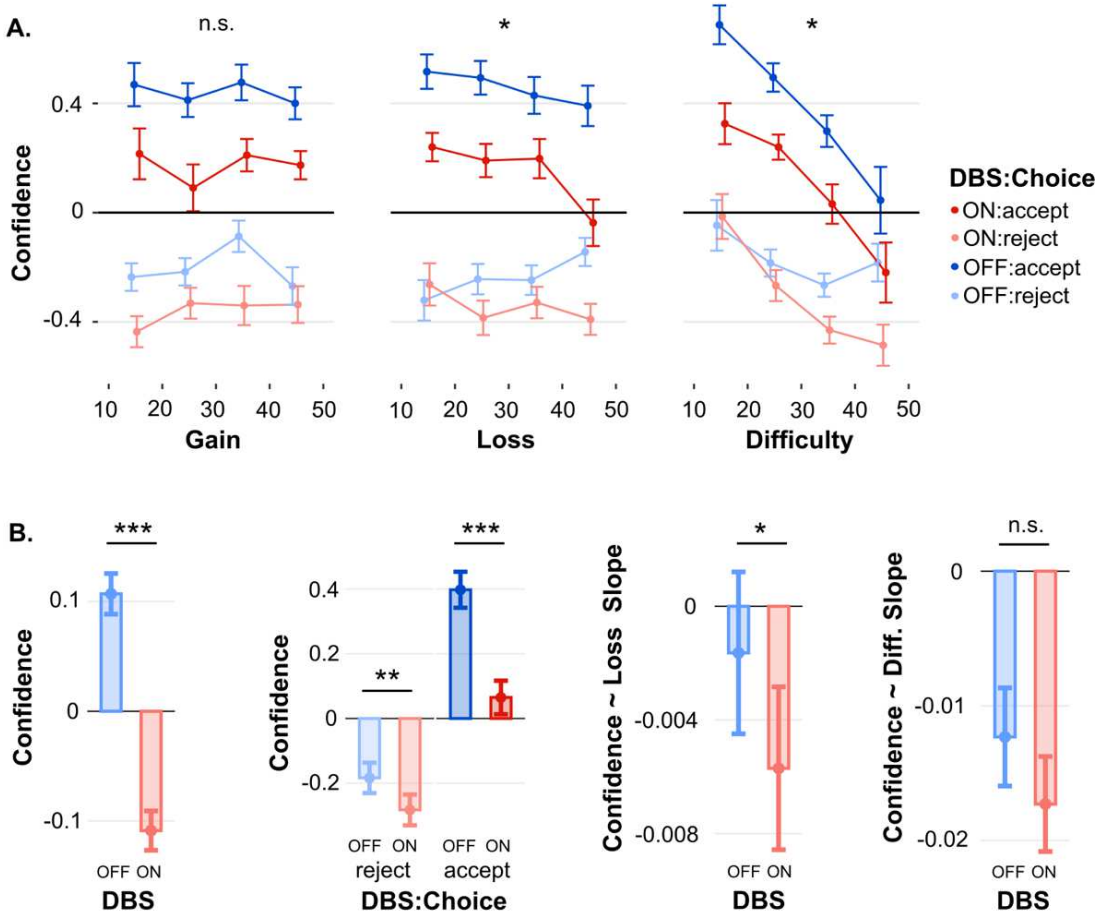


Figure 3. avmSTN DBS reduces prospective confidence in challenge success. A. Normalized (z-scored) prospective confidence plotted as a function of offer attributes and choice. Dots and error bars show binned data, averaged across participants ± SEM for gain prospect, loss prospect and challenge difficulty, separately according to accept/reject choice. Statistical effects were assessed using the linear mixed-effects model reported in Table S5. **B.** Effect of avmSTN DBS on prospective confidence. Estimated marginal means showed lower prospective confidence during DBS ON than OFF, with a larger DBS-related decrease for accepted than rejected challenges. The mixed effects model further showed DBS × loss prospect and DBS × challenge difficulty interactions, whereas the corresponding marginal comparisons of slopes between DBS conditions reached significance only for loss (Table S6). For the two left panels, points and error bars show estimated marginal means ± SEM. The right panels show estimated marginal trends ± SEM for the relationship between prospective confidence and loss prospect or challenge difficulty. Asterisks indicate post-hoc contrasts: * for $p < 5 \times 10^{-2}$, ** for $p < 10^{-2}$, *** for $p < 10^{-3}$.

avmSTN-DBS strengthens the coupling between feedback and mood

We examined the effect of avmSTN-DBS on reported mood using a mixed-effects model including stimulation condition, feedback received on the preceding trial, and their interaction. DBS had no significant main effect on mood ratings (mean mood ON = 57.0 ± 3.75, mean OFF = 54.8 ± 3.43, effect estimate = 2.12 ± 2.34, t(12) = 0.91, p = 0.38). In contrast, there was a significant stimulation × feedback interaction ($\beta = 6.67 \times 10^{-2} \pm 2.72 \times 10^{-2}$, $t_{(1692)} = 2.45$, $p = 1.45 \times 10^{-2}$, **Fig. 4A; Table S7**). Mood increased with more positive feedback in both stimulation conditions, but the feedback–mood relationship was steeper during DBS ON ($\beta = 0.250 \pm 0.019$) than during DBS OFF ($\beta = 0.184 \pm 0.019$). Accordingly, the difference between slopes was significant ($\Delta\beta = 6.67 \times 10^{-2}$, $t_{(1692)} = 2.45$, $p = 1.45 \times 10^{-2}$; **Fig. 4B; Table S8**). Thus, avmSTN-DBS did not produce an overall change in reported mood but increased the sensitivity of momentary mood ratings to recent feedback.

We next used a computational model of mood fluctuations validated previously in healthy subjects or in epileptic patients during invasive electrophysiological recordings [22,23] to estimate a continuous theoretical mood level (TML) across trials. The model uses intermittent mood ratings together with the recent history of feedback to estimate trial-by-trial fluctuations in mood (see methods). Because successive TML estimates are temporally dependent, we tested the effect of stimulation on TML using a linear mixed-effects model that accounted for correlations between successive trials and included participant-specific random intercepts. This analysis revealed significantly higher TML during DBS ON than DBS OFF ($\beta = 2.16 \times 10^{-1} \pm 8.15 \times 10^{-2}$, $t_{(6834)} = 2.65$, $p = 8.13 \times 10^{-3}$; **Fig. 4C**). Estimated marginal TML was higher during DBS ON than DBS OFF (ON: $1.32 \times 10^{-1} \pm 5.70 \times 10^{-2}$; OFF: $-8.44 \times 10^{-2} \pm 5.79 \times 10^{-2}$), corresponding to an estimated ON–OFF difference of 2.16×10^{-1}. However, this effect was sensitive to the specification of inter-individual variability: in a control analysis additionally allowing the effect of stimulation to vary across participants, the estimated DBS effect remained similar in magnitude ($\beta = 2.02 \times 10^{-1}$) but its uncertainty increased substantially (1.80×10^{-1}), and the effect was no longer significant ($t_{(6834)} = 1.12$, $p = 0.263$). Thus, although the primary analysis indicated an increase in TML during DBS, the robustness of this effect across participants was limited. Finally, we tested whether DBS altered the parameters of the computational mood model. The model was fitted separately for each participant in the DBS ON and OFF conditions, and the resulting parameter estimates were compared within participants using paired two-sided *t*-tests. None of the model parameters differed significantly between stimulation conditions (all $p > 0.1$; **Table S9**), providing no evidence that DBS systematically altered the computational parameters governing mood dynamics.

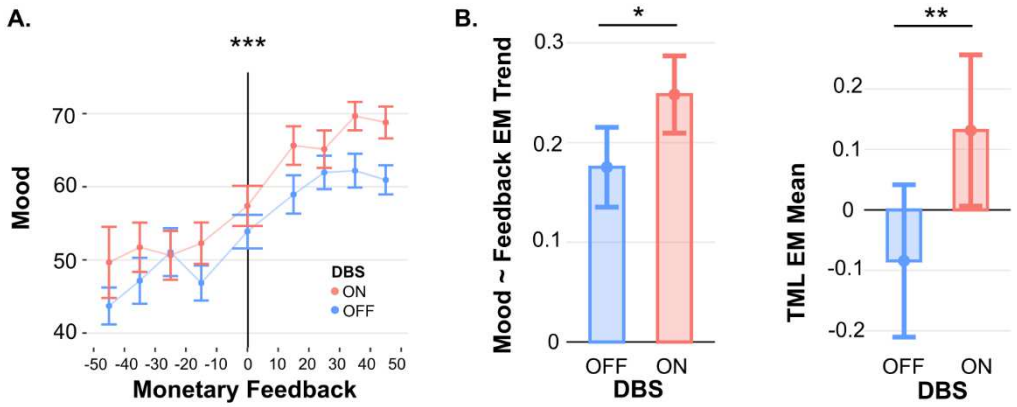


Figure 4. avmSTN-DBS increases the sensitivity of mood to feedback. A. Mood ratings in OCD patients as a function of stimulation condition (DBS ON or OFF) and monetary feedback. For visualization, feedback values were grouped into 10-cent bins. Dots and error bars represent the across-participant mean ± SEM. B. Interaction between DBS and feedback on mood ratings, as extracted from the GLMM. Dots and error bars represent model-estimated marginal means ± SEM. The feedback–mood relationship was significantly steeper during DBS ON than DBS OFF (DBS × feedback interaction, p = 0.0145), indicating increased sensitivity of momentary mood to feedback during stimulation. C. Effect of DBS on theoretical mood level (TML), as extracted from the GLMM with autocorrelation. Dots and error bars represent estimated marginal TML ± SEM from the primary mixed-effects model accounting for temporal dependence between successive trials and participant-specific random intercepts. TML was significantly higher during DBS ON than DBS OFF in this analysis (p = 0.0081). This effect was not significant in a control model additionally allowing the effect of stimulation to vary across participants.

DISCUSSION

Here, we examined the effects of avmSTN-DBS on choice behavior, prospective confidence, and mood in patients with OCD. We found that avmSTN stimulation reduced the weight assigned to prospective losses during risky decisions. It also decreased prospective confidence, while increasing mood and strengthening the influence of recent monetary feedback on mood. This apparently paradoxical pattern is noteworthy given the typically positive relationship between confidence and affect. Together, these findings suggest that avmSTN stimulation can differentially influence the evaluation of prospective negative outcomes, confidence about future performance, and the affective impact of recent outcomes. In the following, we discuss how these findings may help clarify the contribution of the avmSTN to valuation, prospective confidence, and affective processing, and how these effects may relate to the pathophysiology of OCD.

A prominent account of OCD emphasizes the disproportionate influence of anticipated aversive consequences on behavior, including enhanced vigilance toward negative outcomes, avoidance, and altered learning from threat and safety signals [3,24,25]. Although our task does not probe aversive conditioning or avoidance directly, monetary losses provide a controlled way of assessing how prospective negative consequences influence choice. OCD patients have been reported to show enhanced learning from loss outcomes and a valence-dependent imbalance in learning from positive and negative outcomes [25,26]. Here, we found that avmSTN-DBS reduced the weight patients assigned to prospective monetary losses during risky choice. This finding is consistent with our previous work showing that stimulation of the same associative-limbic STN target impaired discrimination of loss magnitude during risk anticipation in OCD patients [16]. Together, these findings converge on a role of the avmSTN in determining how prospective negative outcomes influence choice.

A possible, though speculative, mechanism is that avmSTN-DBS modulates a network involved in aversive valuation. The anterior insula is implicated in the weighting of prospective losses in both neuroimaging and intracranial studies [22,23] and shows altered responses to aversive stimuli in OCD [27]. Given its anatomical connectivity with the STN [28], modulation of an insula–avmSTN circuit could contribute to the reduced loss weighting observed here.

avmSTN-DBS also produced a marked change in prospective confidence, lowering patients' confidence in their ability to succeed in the upcoming cognitive challenge while strengthening its trial-by-trial dependence on task difficulty and prospective loss. This pattern suggests that stimulation does not simply blunt metacognitive evaluation, but rather shifts the overall level of prospective confidence while preserving its sensitivity to task-relevant information. This finding is particularly relevant in OCD, where low confidence and doubt are closely linked to symptom expression. In a large momentary-assessment study, transient decreases in self-confidence and in task-based metacognitive bias preceded subsequent symptom episodes [29]. More generally, underconfidence has been reported across different levels of metacognitive judgment in OCD [30]. Against this background, a reduction in confidence under effective DBS may appear counterintuitive. However, Kiverstein et al. [31] explicitly proposed that the effects of DBS on self-confidence may depend on the stimulation target. They argued that, compared with vALIC stimulation, STN stimulation may reduce compulsivity while exerting weaker effects on anxiety, predicting that self-confidence could therefore remain relatively low under STN-DBS. Our finding is consistent with this target-specific prediction. The decrease observed here also contrasts with the absence of an effect of avmSTN-DBS on retrospective confidence

during perceptual decisions in the same cohort [32], suggesting that stimulation may affect different forms of confidence differently. Moreover, the coexistence of lower average confidence with stronger modulation by task difficulty and prospective loss is reminiscent of recent findings showing that OCD patients can exhibit globally reduced confidence while their confidence judgments remain highly sensitive to task-relevant evidence [33]. Thus, lower prospective confidence under stimulation need not imply a nonspecific impairment of metacognitive evaluation.

This pattern could arise if avmSTN-DBS lowers the amount of evidence needed to reach a decision, rather than increasing subjective certainty itself. The STN transiently raises decision thresholds under conflict, an effect disrupted by STN stimulation [34]. In OCD, STN neuronal activity has also been linked to checking behavior [17]. Our previous work showed that stimulation of the same associative-limbic STN target reduced evidence accumulation under uncertainty [15]. Within this framework, reaching decisions with less accumulated evidence could lower subsequent prospective confidence. The simultaneous reduction in loss weighing observed here is also consistent with a reduced behavioral impact of potential negative consequences. This interpretation converges with our previous finding that stimulation impaired discrimination of loss magnitude during risk anticipation (Voon et al., 2018). Thus, avmSTN-DBS may not resolve uncertainty itself, but reduce the extent to which uncertainty and prospective negative consequences shape choice.

avmSTN-DBS also altered mood dynamics, most notably by strengthening the influence of recent monetary feedback on mood. This extends previous evidence that stimulation of the same associative-limbic STN target modulates affective evaluation in OCD. In particular, avmSTN-DBS shifted ratings of low-intensity emotional stimuli toward more positive evaluations, an effect proposed to reflect altered processing when affective information is ambiguous or uncertain [19]. Consistent with this, STN stimulation has repeatedly been shown to modulate affective state in Parkinson's disease, ranging from changes in mood to stimulation-induced hypomania following anteromedial STN [35–41]. The stronger coupling between feedback and mood observed here further suggests that avmSTN-DBS alters how strongly recent outcomes shape moment-to-moment affective state, consistent with computational accounts in which mood reflects the integration of recent feedback history [21–23]. Together, these findings support a role of the associative-limbic STN in modulating both affective state and its sensitivity to recent outcomes.

Several limitations should be considered when interpreting these findings. First, patients had received chronic avmSTN stimulation for at least one year before testing; the acute OFF condition therefore cannot be considered an untreated baseline and may include withdrawal, residual stimulation, or compensatory effects. Second, the modest sample size limits the ability to identify reliable between-subject relationships between cognitive, affective, and clinical effects of stimulation. Direct comparisons with healthy participants are also constrained by differences in challenge performance. Despite these limitations, our findings provide converging evidence that avmSTN-DBS influences several components of value-based behavior in OCD: the weighting of prospective losses, the formation of prospective confidence, and the impact of recent outcomes on affective state. Together with previous work from the same target, these results support a causal role of the associative-limbic STN in regulating how prospective consequences and uncertainty shape choice, confidence, and affect. Future studies combining computational modeling, precise contact localization, and larger cohorts will be important to determine how these behavioral effects relate to therapeutic response.

MATERIALS AND METHODS

Participants and clinical evaluation

Seventeen patients meeting DSM-IV criteria for severe, treatment-refractory obsessive–compulsive disorder (OCD) were recruited from the STN-DBS clinical trial conducted at Grenoble Alpes University Hospital (NCT02844049). As part of this trial, patients had been implanted bilaterally with 8-contact directional DBS electrodes (Boston Scientific, Marlborough, MA, USA) targeting the antero-ventro-medial subthalamic nucleus (avmSTN) and had received chronic stimulation for at least 12 months before the present experiment. Four patients were excluded from the behavioral analyses: one completed only one experimental session, and three were unable to complete the task because of sleepiness or OCD symptoms. The final patient sample therefore comprised 13 participants with OCD (10 women; mean age, 43.8 years; **Table S1**). The clinical protocol was approved by the CPP Sud-Est V ethics committee (2012-A00490-43/5), and all participants provided written informed consent. Eighteen healthy control participants were recruited separately. Participants reported no current or past neurological or psychiatric disorder and had normal or corrected-to-normal vision. One participant was excluded because of a technical problem, resulting in a final control sample of 17 participants (13 women; mean age, 45.5 years). The control protocol was approved by the

Grenoble Alpes University Research Ethics Committee (CER Grenoble Alpes, Avis-2019-11-05-4), and all participants provided written informed consent.

General cognitive functioning was assessed using the Addenbrooke's Cognitive Examination–Revised (ACE-R; [42]). Control participants were assessed at inclusion in the present study, whereas patients with OCD had been assessed at inclusion in the DBS clinical protocol; only participants with an ACE-R score ≥80 were included. Long-term clinical effects of avmSTN-DBS on OCD symptoms were assessed using the Yale–Brown Obsessive Compulsive Scale (Y-BOCS; [43,44]). Total Y-BOCS scores obtained before DBS implantation were compared with scores obtained during the initial clinical evaluation on day 0 of the present experiment, while patients were receiving their chronic stimulation and before any experimental manipulation of DBS. To assess short-term changes in clinical state associated with stimulation withdrawal, Y-BOCS Resistance and Control items, anxiety symptoms assessed with the Beck Anxiety Inventory (BAI; [45]), and depressive symptoms assessed with the Beck Depression Inventory–Fast Screen (BDI-FS; [46]) were measured in both DBS ON and OFF conditions.

Procedure and behavioral task

Patients with OCD completed the experiment in two stimulation conditions, with avmSTN-DBS either ON or OFF, using a randomized, double-blind, counterbalanced crossover design (**Fig. 1A**). The two experimental sessions were conducted on consecutive days and separated by a 16-h washout period, following a procedure previously used to minimize carry-over effects of stimulation [47]. Participants and experimenters administering the behavioral task were blind to the stimulation condition. Participants performed a previously validated accept/reject task adapted to assess choice, prospective confidence and mood within the same experimental session [22,23,48]. Each session comprised 3–5 blocks of 64 trials, corresponding to 192–320 trials and approximately 1 h of testing. Each trial consisted of a choice, a prospective confidence rating, a cognitive challenge and monetary feedback; a mood rating was additionally collected on 25% of trials (**Fig. 1D**).

Control participants were trained immediately before the experimental session. Patients with OCD completed the training on day 0, while receiving chronic DBS, after the initial clinical evaluation and before any experimental manipulation of stimulation (**Fig. 1A**). Training first familiarized participants with the challenge and then with the complete task. Participants initially performed 28 challenge trials with feedback indicating whether their response was correct, too early or too late; an additional 28 trials were administered when performance was

below 50%. They subsequently completed 64 trials of the full task, including choice, challenge and monetary feedback. During this phase, challenge difficulty progressively increased to facilitate learning of the relationship between target size and probability of success. Challenge difficulty was individually calibrated from each participant's temporal estimation errors during training. Assuming a Gaussian distribution of these errors, target widths were adjusted to define five difficulty levels corresponding to theoretical success probabilities ranging from 75% for the easiest level to 35% for the hardest. Estimates of individual performance variability were updated throughout training and then fixed at the end of the training phase to determine the target sizes used during the experimental sessions.

During the choice phase, participants were presented with an offer defined by three attributes: a potential monetary gain, a potential monetary loss and the difficulty of the upcoming challenge. Gain and loss magnitudes ranged from 10 to 50 coins, with each coin corresponding to €0.10. Challenge difficulty was manipulated by varying the size of the target and was individually calibrated before testing. Participants decided whether to accept or reject the offer. If accepted, successful completion of the subsequent challenge resulted in the displayed gain, whereas failure resulted in the displayed loss. If the offer was rejected, participants still performed the same challenge but for minimal stakes of €0.10 for either success or failure. Thus, rejecting an offer reduced the monetary consequences without avoiding the cognitive challenge. Participants were instructed to try to maximize monetary gains and minimize monetary losses.

Immediately after each choice, participants rated their prospective confidence in successfully completing the upcoming challenge by answering the question "Do you think you are going to win?" on a visual analog scale ranging from "Not sure" to "Sure". Participants then performed the challenge. A ball moved horizontally toward a target located at the center of the screen. Its trajectory was visible for the first 500 ms and then occluded for the subsequent 500 ms, during which participants extrapolated its movement and pressed a response button when they estimated that the ball had reached the target. A trial was considered successful when the response occurred within the target window. Target size was varied to manipulate challenge difficulty. Following the response, participants received visual feedback indicating whether the challenge had been successfully completed and the corresponding monetary outcome. On 25% of trials, participants subsequently rated their current mood by answering "How do you feel right now?" on a visual analog scale ranging from "Very bad" to "Very good". Participants were instructed to use their mood at the beginning of the first block as the midpoint reference. The initial cursor position was randomized across ratings. Mood was sampled on a subset of

trials to limit repeated self-assessment while allowing mood fluctuations to develop across the session.

Electrodes anatomical localization reconstruction

We used the Lead-DBS image reconstruction Matlab toolkit [49,50] to coregister preoperative MRI with post-operative CT scans. For each patient, we used advanced normalization tools ANTs [51–53] to co-register preoperative T1-weighted 3D images with postoperative CT, including a correction for brainshift during surgery using the default option 'coarse mask' [54]. Then, based on the preoperative volumes, we used the non-linear segmentation method [55] of the Statistical Parametric Mapping SPM12 [56,57] to compute a multispectral normalization in the asymmetric nonlinear space ICBM 2009b [58]. Then, the PaCER method was applied to automatically reconstruct the DBS electrodes and their directional contacts [59]. To determine the location of each electrode contact relative to STN subdivisions, we segmented the reconstructed images using the DISTAL atlas [60]. Finally, we reconstructed the position of all pairs of electrodes in **Fig. 1C**.

Behavioral analyses of choice and prospective confidence

All analyses were conducted in R version 4.4.0 (R Core Team, 2024) using the lme4 package [61] version 1.1.35.5 for linear mixed-effects models and the emmeans package [62] for estimated marginal means and post-hoc contrasts. Statistical significance was assessed at $P < 0.05$. All statistical tests were two-sided.

Choice (accept/reject) was analyzed using a generalized linear mixed-effects model with a binomial distribution and logit link. Gain, loss, challenge difficulty and stimulation were entered as fixed effects, together with the interaction between stimulation and each task variable. Participant-specific random intercepts and random slopes for stimulation were included:

$$\text{Accept} \sim (gain + loss + difficulty) \times stimulation + (1 + stimulation \mid participant)$$

Prospective confidence in challenge success was defined as the participant's prospective subjective rating, before performing the challenge, of the likelihood of succeeding. Trial-by-trial prospective confidence ratings were z-scored and analyzed using a linear mixed-effects model including gain, loss, challenge difficulty, choice (accept/reject), stimulation, and all interactions between these factors as fixed effects. A participant-specific random intercept

was included; random slopes were not retained because the corresponding models failed to converge:

$$z(confidence) \sim (gain + loss + difficulty) \times accept \times stimulation + (1|participant)$$

Estimated marginal means and pairwise contrasts were obtained using the emmeans package. Contrasts were evaluated using asymptotic Wald z-tests.

Computational model of choice behavior

To characterize choice behavior, we used a previously validated computational model [22]. The model is based on expected utility theory and captures the influence of prospective gains and losses on choice through separate weighting parameters (k_g and k_l respectively). It further includes a temporal drift parameter (k_t), a constant bias term (k_0), and a parameter σ capturing uncertainty in the internal representation of challenge performance.

For each trial, expected utility was determined by the potential gain (*G*) and loss (*L*), weighted by the subjective probability of succeeding at the challenge (*p*s). The probability of accepting an offer was then modeled as a sigmoid function of expected utility and a linear temporal drift term:

$$p(accept, t) = \frac{1}{1 + e^{-(utility + k_t \times t)}}$$

where *t* denotes trial index and k_t captures a linear drift in choice over time, allowing for systematic changes across the session.

The utility function is based on expected utility theory where potential gains and losses are multiplied by probability of success (p_s) vs. failure ($1 - p_s$):

$$utility = k_0 + p_s \times k_g \times gain - (1 - p_s) \times k_l \times loss$$

where *k*g and *k*l capture the respective influence of prospective gains and losses on choice, and *k*0 captures an overall choice bias.

The subjective probability of success (p_s) was determined jointly by target size and the participant's assumed uncertainty about challenge performance. The model assumes that challenge performance is represented by a Gaussian distribution centered on the target value (1 s), with its width determined by the free parameter (σ). For a target window of width (*size*), success corresponds to performance falling between (1- *size* /2) and (1+ *size* /2). Accordingly,

the subjective probability of success was computed as the probability mass of this Gaussian distribution falling within the target window:

$$p_s = \frac{1}{\sigma\sqrt{2\pi}} \int_{1-size/2}^{1+size/2} e^{\frac{-(x-1)^2}{2\sigma^2}} dx$$

Thus, larger target windows yield higher subjective probabilities of success, whereas σ captures uncertainty in the internal representation of challenge performance.

Choice models were fitted for each participant and DBS condition separately, using MATLAB (R2021b, The MathWorks, Inc, USA) and the VBA toolbox available at https://mbb-team.github.io/VBA-toolbox/ [63].

All the choice model parameters were compared between conditions using paired T-tests.

Computational modeling of mood fluctuations

To characterize trial-by-trial mood fluctuations and the reciprocal influence between mood and challenge feedback, we fitted a previously published computational mood model[22,23]. The model yielded a Theoretical Mood Level (TML) for each trial and included a baseline parameter (k_0), a temporal drift parameter (k_t), a feedback-weight parameter (k_F), a forgetting factor (γ), a parameter capturing the influence of prior mood on feedback perception (k_{mood}), and a parameter allowing asymmetric effects of positive and negative feedback (*R*). The TML at trial *t* was defined as:

$$TML(t) = k_0 + k_f \sum_{j=1}^{t} \gamma^{t-j} F(j) + k_t t$$

where *t* denotes trial index, k_0 captures baseline mood, k_F determines the influence of feedback on mood, and k_t captures a linear change in mood over the course of the session. The forgetting factor γ ($0 \leq \gamma \leq 1$) determines the relative influence of recent versus more distant feedback, with lower values producing a faster decay of past feedback effects. F is the subjective perception of feedback. This formulation corresponds to the feedback-integration model used previously to reconstruct trial-by-trial mood fluctuations.

The model further allowed positive and negative feedback to exert asymmetric effects on mood. Objective feedback was coded as R following positive feedback and −1 following negative feedback, with R>0 estimated as a free parameter. Objective feedback was then transformed into subjective feedback, F(t), by incorporating the influence of mood carried over from the preceding trial:

$$F(t) = Feedback(t) + k_m \times TML(t-1)$$

where k_m is a free parameter capturing the influence of prior mood on feedback perception, and TML(t−1) represents mood before incorporation of the feedback received on the current trial. Thus, higher mood shifted the subjective perception of subsequent feedback in a more positive direction, whereas lower mood shifted it in a more negative direction. Similarly to the choice model, the mood model was inverted with Matlab R2021b using the Matlab VBA toolbox separately for each participant and condition. We then extracted the model parameters for each participant, in each condition, and compared the parameters between conditions using T-tests.

Finally, TML at each trial was analyzed using a linear mixed-effects model with session (DBS status) as a fixed effect and a subject-specific random intercept. To account for within-subject, within-session temporal dependence, we specified a first-order autoregressive [AR(1)] correlation structure for the residuals, indexed by trial number separately for each subject and session. The model was fitted using the nlme package in R.

$$TML \sim stimulation + (1|participant) + AR(1)_{trial|participant/stimulation}$$

Data availability

The behavioral data generated in this study will be deposited in OSF. Source data are provided with this paper.

Code availability

All Matlab code necessary to reproduce our analyses will be made available, without restriction at OSF.

REFERENCES

1. Abramowitz, J. S., Taylor, S. & McKay, D. Obsessive-compulsive disorder. *The Lancet* **374**, 491–499 (2009).
2. Mallet, L. *et al.* Subthalamic Nucleus Stimulation in Severe Obsessive–Compulsive Disorder. *N Engl J Med* **359**, 2121–2134 (2008).
3. Cui, H. *et al.* Mechanisms underlying capsulotomy for refractory obsessive-compulsive disorder: neural correlates of negative affect processing overlap with deep brain stimulation targets. *Mol Psychiatry* **28**, 3063–3074 (2023).
4. Dar, R., Sarna, N., Yardeni, G. & Lazarov, A. Are people with obsessive-compulsive disorder under-confident in their memory and perception? A review and meta-analysis. *Psychological Medicine* 1–9 (2022) doi:10.1017/S0033291722001908.
5. George, S. A., Sheynin, J., Gonzalez, R., Liberzon, I. & Abelson, J. L. Diminished Value Discrimination in Obsessive-Compulsive Disorder: A Prospect Theory Model of Decision-Making Under Risk. *Frontiers in Psychiatry* **10**, (2019).
6. Hoven, M. *et al.* Abnormalities of confidence in psychiatry: an overview and future perspectives. *Transl Psychiatry* **9**, 268 (2019).
7. Hoy, C. W. *et al.* Beta and theta oscillations track effort and previous reward in the human basal ganglia and prefrontal cortex during decision making. *Proceedings of the National Academy of Sciences* **121**, e2322869121 (2024).
8. Zénon, A. *et al.* The human subthalamic nucleus encodes the subjective value of reward and the cost of effort during decision-making. *Brain* **139**, 1830–1843 (2016).
9. Atkinson-Clement, C. *et al.* Effects of subthalamic nucleus stimulation and levodopa on decision-making in Parkinson's disease. *Mov Disord.* **34**, 377–385 (2019).
10. Patel, S. R. *et al.* Intermittent subthalamic nucleus deep brain stimulation induces risk-aversive behavior in human subjects. *eLife* **7**, e36460 (2018).
11. Voon, V. *et al.* Modeling impulsivity and risk aversion in the subthalamic nucleus with deep brain stimulation. *Nat. Mental Health* **2**, 1084–1095 (2024).

12. Krack, P. *et al.* Mirthful laughter induced by subthalamic nucleus stimulation. *Mov Disord* **16**, 867–875 (2001).
13. Hollunder, B. *et al.* Mapping dysfunctional circuits in the frontal cortex using deep brain stimulation. *Nat Neurosci* 1–14 (2024) doi:10.1038/s41593-024-01570-1.
14. Mulders, A. E. P. *et al.* Deep brain stimulation of the subthalamic nucleus in obsessive-compulsive disorder: Neuroanatomical and pathophysiological considerations. *European Neuropsychopharmacology* **26**, 1909–1919 (2016).
15. Voon, V. *et al.* Decisional impulsivity and the associative-limbic subthalamic nucleus in obsessive-compulsive disorder: stimulation and connectivity. *Brain* **140**, 442–456 (2017).
16. Voon, V. *et al.* Dissociable Effects of Subthalamic Stimulation in Obsessive Compulsive Disorder on Risky Reward and Loss Prospects. *Neuroscience* **382**, 105–114 (2018).
17. Burbaud, P. *et al.* Neuronal activity correlated with checking behaviour in the subthalamic nucleus of patients with obsessive–compulsive disorder. *Brain* **136**, 304–317 (2013).
18. Buot, A. *et al.* Emotions Modulate Subthalamic Nucleus Activity: New Evidence in Obsessive-Compulsive Disorder and Parkinson's Disease Patients. *Biol Psychiatry Cogn Neurosci Neuroimaging* **6**, 556–567 (2021).
19. Polosan, M. *et al.* Affective modulation of the associative-limbic subthalamic nucleus: deep brain stimulation in obsessive–compulsive disorder. *Transl Psychiatry* **9**, 73 (2019).
20. Eldar, E. & Niv, Y. Interaction between emotional state and learning underlies mood instability. *Nat Commun* **6**, 6149 (2015).
21. Rutledge, R. B., Skandali, N., Dayan, P. & Dolan, R. J. A computational and neural model of momentary subjective well-being. *Proceedings of the National Academy of Sciences* **111**, 12252–12257 (2014).
22. Vinckier, F., Rigoux, L., Oudiette, D. & Pessiglione, M. Neuro-computational account of how mood fluctuations arise and affect decision making. *Nat Commun* **9**, 1708 (2018).
23. Cecchi, R. *et al.* Intracerebral mechanisms explaining the impact of incidental feedback on mood state and risky choice. *eLife* **11**, e72440 (2022).

24. Gillan, C. M. & Robbins, T. W. Goal-directed learning and obsessive-compulsive disorder. *Philos Trans R Soc Lond B Biol Sci* **369**, 20130475 (2014).
25. Voon, V. *et al.* Risk-taking in disorders of natural and drug rewards: neural correlates and effects of probability, valence, and magnitude. *Neuropsychopharmacology* **40**, 804–812 (2015).
26. Sakai, Y., Sakai, Y., Abe, Y., Narumoto, J. & Tanaka, S. C. Memory trace imbalance in reinforcement and punishment systems can reinforce implicit choices leading to obsessive-compulsive behavior. *Cell Reports* **40**, 111275 (2022).
27. Berlin, H. A. *et al.* Altered olfactory processing and increased insula activity in patients with obsessive-compulsive disorder: an fMRI study. *Psychiatry Res* **262**, 15–24 (2017).
28. Lambert, C. *et al.* Confirmation of functional zones within the human subthalamic nucleus: Patterns of connectivity and sub-parcellation using diffusion weighted imaging. *Neuroimage* **60**, 83–94 (2012).
29. Marzuki, A. A., Kosina, L. A., Dome, L., Hewitt, S. R. C. & Hauser, T. U. Drops in confidence precede symptoms of obsessive-compulsive disorder. *Nat Commun* **17**, 8333 (2026).
30. Hoven, M., Rouault, M., van Holst, R. & Luigjes, J. Differences in metacognitive functioning between obsessive-compulsive disorder patients and highly compulsive individuals from the general population. *Psychol Med* **53**, 7933–7942 (2023).
31. Kiverstein, J., Rietveld, E., Slagter, H. A. & Denys, D. Obsessive Compulsive Disorder: A Pathology of Self-Confidence? *Trends in Cognitive Sciences* **23**, 369–372 (2019).
32. Kist, A. *et al.* Assessing the effect of subthalamic stimulation on metaperception in obsessive-compulsive disorder. *Transl Psychiatry* https://doi.org/10.1038/s41398-026-04423-6 (2026) doi:10.1038/s41398-026-04423-6.
33. Loosen, A. M. *et al.* The metacognitive paradox of OCD: confidence is globally reduced but shows increased sensitivity to local evidence. *Transl Psychiatry* https://doi.org/10.1038/s41398-026-04399-3 (2026) doi:10.1038/s41398-026-04399-3.
34. Cavanagh, J. F. *et al.* Subthalamic nucleus stimulation reverses mediofrontal influence over decision threshold. *Nat Neurosci* **14**, 1462–1467 (2011).

35. Accolla, E. A. & Pollo, C. Mood Effects After Deep Brain Stimulation for Parkinson's Disease: An Update. *Front Neurol* **10**, 617 (2019).
36. Buot, A. *et al.* Processing of emotional information in the human subthalamic nucleus. *Journal of Neurology, Neurosurgery & Psychiatry* **84**, 1331–1339 (2013).
37. Campbell, M. C. *et al.* Mood Response to Deep Brain Stimulation of the Subthalamic Nucleus in Parkinson Disease. *J Neuropsychiatry Clin Neurosci* **24**, 28–36 (2012).
38. Castrioto, A., Lhommée, E., Moro, E. & Krack, P. Mood and behavioural effects of subthalamic stimulation in Parkinson's disease. *The Lancet Neurology* **13**, 287–305 (2014).
39. Mallet, L. *et al.* Stimulation of subterritories of the subthalamic nucleus reveals its role in the integration of the emotional and motor aspects of behavior. *Proc Natl Acad Sci U S A* **104**, 10661–10666 (2007).
40. Okun, M. S. *et al.* Acute and Chronic Mood and Apathy Outcomes from a randomized study of unilateral STN and GPi DBS. *PLoS One* **9**, e114140 (2014).
41. Ricciardi, L., Apps, M. & Little, S. Uncovering the neurophysiology of mood, motivation and behavioral symptoms in Parkinson's disease through intracranial recordings. *npj Parkinsons Dis.* **9**, 1–16 (2023).
42. Mioshi, E., Dawson, K., Mitchell, J., Arnold, R. & Hodges, J. R. The Addenbrooke's Cognitive Examination Revised (ACE-R): a brief cognitive test battery for dementia screening. *Int J Geriatr Psychiatry* **21**, 1078–1085 (2006).
43. Goodman, W. K. *et al.* The Yale-Brown Obsessive Compulsive Scale. II. Validity. *Arch Gen Psychiatry* **46**, 1012–1016 (1989).
44. Mollard, E., Cottraux, J. & Bouvard, M. Version française de l'échelle d'obsession-compulsion de Yale-Brown. / Yale-Brown Obsessive-Compulsive Scale: A French version. *L'Encéphale: Revue de psychiatrie clinique biologique et thérapeutique* **XV**, 335–341 (1989).
45. Beck, A. T., Epstein, N., Brown, G. & Steer, R. A. An inventory for measuring clinical anxiety: Psychometric properties. *Journal of Consulting and Clinical Psychology* **56**, 893–897 (1988).
46. Beck, A. T., Steer, R. A. & Brown, G. K. BDI – FastScreen for Medical Patients. American Psychological Association https://doi.org/10.1037/t14984-000 (2012).

47. Kibleur, A. *et al.* Modulation of motor inhibition by subthalamic stimulation in obsessive-compulsive disorder. *Transl Psychiatry* **6**, e922–e922 (2016).
48. Cecchi, R. *et al.* Direct stimulation of anterior insula and ventromedial prefrontal cortex disrupts economic choices. *Nature Communications* **15**, (2024).
49. Horn, A. *et al.* Lead-DBS v2: Towards a comprehensive pipeline for deep brain stimulation imaging. *NeuroImage* **184**, 293–316 (2019).
50. Horn, A. & Kühn, A. A. Lead-DBS: A toolbox for deep brain stimulation electrode localizations and visualizations. *NeuroImage* **107**, 127–135 (2015).
51. Avants, B., Tustison, N. & Song, G. Advanced Normalization Tools (ANTS). University of Pennsylvania.
52. Avants, B., Tustison, N. J. & Song, G. Advanced Normalization Tools: V1.0. *The Insight Journal* https://doi.org/10.54294/uvnhin (2009) doi:10.54294/uvnhin.
53. Avants, B. B. *et al.* A reproducible evaluation of ANTs similarity metric performance in brain image registration. *Neuroimage* **54**, 2033–2044 (2011).
54. Schönecker, T., Kupsch, A., Kühn, A. A., Schneider, G.-H. & Hoffmann, K.-T. Automated Optimization of Subcortical Cerebral MR Imaging−Atlas Coregistration for Improved Postoperative Electrode Localization in Deep Brain Stimulation. *AJNR Am J Neuroradiol* **30**, 1914–1921 (2009).
55. Ashburner, J. & Friston, K. J. Unified segmentation. *Neuroimage* **26**, 839–851 (2005).
56. *Statistical Parametric Mapping: The Analysis of Funtional Brain Images*. (Elsevier/Academic Press, Amsterdam ; Boston, 2007).
57. Functional Imaging Laboratory. Statistical Parametric Mapping - SPM. University College London.
58. Fonov, V., Evans, A., McKinstry, R., Almli, C. & Collins, D. Unbiased nonlinear average age-appropriate brain templates from birth to adulthood. *NeuroImage* **47**, S102 (2009).
59. Husch, A., V. Petersen, M., Gemmar, P., Goncalves, J. & Hertel, F. PaCER - A fully automated method for electrode trajectory and contact reconstruction in deep brain stimulation. *NeuroImage: Clinical* **17**, 80–89 (2018).

60. Ewert, S. *et al.* Toward defining deep brain stimulation targets in MNI space: A subcortical atlas based on multimodal MRI, histology and structural connectivity. *Neuroimage* **170**, 271–282 (2018).
61. Bates, D., Mächler, M., Bolker, B. & Walker, S. Fitting Linear Mixed-Effects Models Using lme4. *Journal of Statistical Software* **67**, 1–48 (2015).
62. Lenth, R. emmeans: Estimated Marginal Means, aka Least-Squares Means. (2025).
63. Rigoux, L. VBA toolbox. (2019).

Acknowledgements

J.B. is supported by Agence National de la Recherche (EPICOG: ANR-22-CE17-0057) and Fondation pour la recherché medicale (FRM). We want to thank all the participants in our study. We also thank Margaux Pourady for her work on Figure 1C and Clarissa Baratin for her help on the code.

Author contributions

AK recruited control participants, collected and analyzed the data and wrote the original article with JB. RC coded the task and provided support on analyses. EB and AP took part in the data collection. NF and MPe provided technical and scientific support. SC performed the surgeries. MPo recruited participants and supervised all clinical aspects of the study. JB supervised scientific aspects of the study, designed the task and wrote the article with AK. All authors critically assessed and discussed the results, and revised and approved the manuscript at all stages.

Competing interests

The authors declare no competing interests.

Supplementary Files

This is a list of supplementary files associated with this preprint. Click to download.

- KistNN2026SIJB.docx